



# Kinetics of uranium adsorption from sulfate medium by a commercial anion exchanger modified with quinoline and silicate

Ahmad A. Ahmad<sup>1</sup>

Received: 25 February 2020 / Published online: 9 May 2020  
© Akadémiai Kiadó, Budapest, Hungary 2020

## Abstract

Quinoline Silicate Lewatit Composite and activated Lewatit were prepared and tested for uranium removal from sulfate solution. Uranium sorption capabilities of the tested adsorbents was estimated under different conditions; uranium initial concentration, pH, contact time, temperature, adsorbent dose and interfering ions. Experimental data obeyed Langmuir isotherm model with 69.44 mg/g and 217.39 mg/g theoretical capacity for AL and QSLC, respectively. Thermodynamic studies indicated an exothermic behavior with a decrease in randomness. Kinetics studies showed that the adsorption process obeyed pseudo-second order model. Optimum conditions were carried out for uranium recovery from a rock sample, producing uranium concentrate with 93.33% purity.

**Keywords** Adsorption · Uranium · Quinoline silicate lewatit composite · Elution

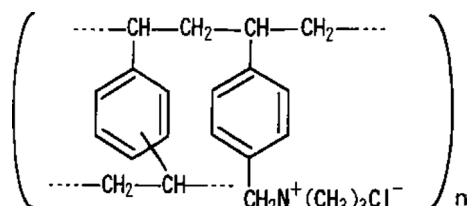
## Introduction

Many types of ion exchange resins have been tried for separation of uranium. So far, strong base anion exchange resins (SBA) are widely used across the world to extract natural uranium (both type I and type II) [1–4]. Though some authors advocate different performance of these two resin types, there wasn't any observed meaningful difference between them [5, 6].

In recent years, a number of strong base anion Lewatit commercial resins, such as Lewatit MP 62 (WBA) [7], Lewatit DW 630 [8], Lewatit S4528 [9], Lewatit K6362 [10], Lewatit K6267 [11], Lewatit MP-64 (WBA) [12, 13], Lewatit MonoPlus M 500 [14–16], Lewatit MonoPlus M 800 [5] and Lewatit MonoPlus M 600 [17] have been used for heavy metals uptake.

Lewatit MonoPlus M 500 is a strongly basic anion exchange resin containing styrene/divinylbenzene copolymer coupled with quaternary ammonium groups. The effective ion exchange capacity is due to the presence of positively charged quaternary amine groups within the polymer skeleton. It is a typical microporous anion exchanger having

about 8% DVB cross-linking that provides both mechanical strength and easy diffusion of exchangeable ions [18]. Its primary structure can be represented by the following formula:



However, the exact structural formula of the resin is cross-linked, irregularly assembled and of much complicated stereostructure [11].

In the following study, the author examines the possibility of integrating the chelating capabilities of quinoline and sodium metasilicate with adsorptive capabilities of Lewatit MonoPlus M 500. The selective separation of uranium from aqueous acidic solution using a new synthesized Lewatit modified with quinoline and sodium metasilicate was studied extensively.

High-capacity composites obtained by modifying Lewatit ion-exchange resins can possess almost two fold the absorption kinetics on them [19]. Adsorption of uranium using quinoline anchored on polymeric resins has been recently

✉ Ahmad A. Ahmad  
zarginah@gmail.com

<sup>1</sup> Nuclear Materials Authority, PO Box 530, Cairo, Maadi, Egypt

studied. The synthesized chelating polymeric sorbent affinity for U (VI) was superior [20]; showing a maximum sorption capacity of 120.30 mg/g. In A study to test the efficiency of adsorption of uranyl ions by cross-linked chitosan resins modified with quinoline-8-ol moiety [21]. The retention capacity found for uranium (VI) was 218 mg/g by the modified resin.

Sodium silicate has shown excellent potential in the safe disposal of radioactive waste due to its special structure and excellent performance [22]. Unfortunately, sodium metasilicate  $\text{Na}_2\text{SiO}_3 \cdot 5\text{H}_2\text{O}$  is soluble in aqueous solution and be easily lost within the medium during batch adsorption experiments. Sodium silicate was successfully integrated with polyacrylic acid as well as tartaric acid to produce novel adsorbents tested and applied for efficient uranium uptake [23]. The advantages of silicate based adsorbents are due to the presence of various chemical entities that can be used for ion-exchange. Its low cost, availability, and environment-friendly nature gave rise to increasing interest in the development of silicate-based adsorbents of ultimate adsorption capacity [24]. Such adsorbents exhibit a quick and highly efficient adsorption behavior toward heavy metal ions [25].

This work focuses on the selective separation of uranium from aqueous acidic solution using a new synthesized composite of Lewatit modified with quinoline and sodium metasilicate. The obtained results were applied to adsorption isotherms and kinetics models. The results demonstrate that the synthesized composite has high uranium removal efficiency and can be physically separated from the treated aqueous solution.

## Experimental

### Instrumentation

The absorbance of uranium,  $\text{SiO}_2$ ,  $\text{Al}_2\text{O}_3$ ,  $\text{TiO}_2$ , and  $\text{P}_2\text{O}_5$  was measured using Metertech SP-8001 UV–visible spectrophotometer.  $\text{Na}^+$  and  $\text{K}^+$  were determined by Sherwood 410 flame photometer. CaO, MgO and total iron content were determined volumetrically [26]. Trace elements and the resulted uranium concentrate from Gattar leach liquor were detected using ICP-OES [27].

The molecular functional groups of AL and QSLC were characterized using Thermo Scientific NICOLET IS10 FTIR spectrometer, before and after uranium adsorption. Scanning electron microscope (SEM) was used illustrate the surface morphology of AL and QSLC before and after uranium adsorption. AL and QSLC were characterized after uranium adsorption by CHNS elemental analysis. The stoichiometry of the constituents was determined using Philips sequent 2400 XRF; Solid samples were ground to very fine powders then mixed with polyvinyl methacrylate as a binder to

facilitate the pressing process. The mixture was pressed in aluminum sample holder of 40 mm diameter by a pressing machine at 20 psi. The concentrations of Na, Mg, Al, Si, P, S, Cl, K, Ca, Fe, Rh, Zr, U and Pb were measured according to Super-Q quantitative application program.

### Chemicals and reagents

Lewatit Mono-Plus M500 anion exchange resin was used to synthesize AL and QSLC. Its activity is gained from quaternary  $-\text{N}(\text{CH}_3)_3^+$  groups. The resin contains exchangeable  $\text{Cl}^-$  ions. The large fixed porosity of the resin bead structure permits the high adsorptive capacity for large molecules. It has excellent regeneration efficiency based on cross-linked polystyrene, excellent physical stability and high operating capacity. The resin characteristics were illustrated in (Table 1).

All chemicals and reagents used are of analytical grade. HCl,  $\text{H}_2\text{SO}_4$  and  $\text{HNO}_3$  were obtained from POCH S.A. N-phenyl anthranilic acid as well as Arsenazo III were obtained from Merck. Ammonium vanadate, bromine, Urea, KBr and  $\text{FeSO}_4 \cdot 7\text{H}_2\text{O}$  were obtained from Scharlau Chemie.

### Preparation of standard stock solution

A standard stock solution of 1000 mg/L of U (VI) was prepared by dissolving  $\text{UO}_2\text{SO}_4$  crystals in distilled water. Several stock solutions of 1000 mg/L of possible interfering ions were prepared.

### Preparation of gattar leach liquor

Studied granitic ore sample assaying 1400 mg/Kg of uranium was obtained from Gattar area, NE Desert, Egypt. Leaching factors were; time 2 h, 3 M  $\text{H}_2\text{SO}_4$ , – 200 mesh

**Table 1** The physical and chemical characteristics of Lewatit Mono Plus M500

Characteristics	Value
Matrix	Poly styrene
Functional groups	Quaternary amine, type I ( $-\text{N}(\text{CH}_3)_3^+$ )
Appearance form	Yellow coloured beads
Ionic form as shipped	( $\text{Cl}^-$ form)
Total exchange capacity	Minimum 1.30 eq/L
Bulk density (g/L)	690
Mean bead size (mm)	0.62 ( $\pm 0.05$ )
Uniformity coefficient max.	1.1
Maximum operating temperature	70 °C
Chemical stability at pH range	0–14
Volume change $\text{Cl}^- \rightarrow \text{OH}^-$	20%

particle size, 25 °C and solid to liquid ratio 1:3 to verify best uranium leaching efficiency (95%). The final leach liquor contained approximately 443 mg/L of uranium. 3L of leach liquor were stirred with suitable weights of AL and QSLC. Major oxides content was determined spectrophotometrically, while trace elements were detected by ICP-OES. All data are shown in (Tables 2, 3 and 4).

## Synthesis of adsorbents

### Synthesis of activated lewatis AL

20 g of Lewatit Mono-Plus M500 were treated with (1:1) ethanol–water solution then 2 mL of HCl (2 M) were added for 10 h to remove any persisting monomers or impurities. The treated Lewatit was washed with distilled water and dried at 50 °C. The dried Lewatit was placed into a beaker containing 0.5 M oxalic acid and stirred for 4 h then filtered and dried at room temperature for 2 days.

### Synthesis of quinoline silicate lewatis composite QSLC

After preparation of activated Lewatit, 10 g of AL were mixed with 10 g of sodium meta-silicate in 250 ml conical flask containing 50 mL of 2 M quinoline dissolved in toluene and stirred for 4 h. The obtained composite was filtered and washed with 3 M H<sub>2</sub>SO<sub>4</sub> then dried at room temperature for 2 days.

## Adsorption procedures

Factors affecting U (VI) adsorption were studied by two adsorbents AL and QSLC; pH, contact time, initial

uranium concentration, adsorbent dose, temperature and interfering ions. In each experiment, 25 mL of synthetic uranium solution containing uranium concentration 50–700 mg/L were stirred at 150 rpm with 0.05 g of each adsorbent for a definite time from 5 to 60 min at different temperatures. Uranium uptake capacity ( $q_e$ , mg/g) was calculated from the following relation:

$$q_e = (C_o - C_e) \times \left[ \frac{V}{m} \right] \quad (1)$$

where  $C_o$  and  $C_e$  are the initial and uranium concentration at equilibrium (mg/L), respectively.  $V$  is volume of the aqueous solution (L) containing uranium and  $m$  is the adsorbent weight (g). The distribution coefficient  $K_d$  is calculated using Eq. (2), where;  $V$  is the volume of the aqueous phase (mL):

$$K_d = \frac{C_o - C_e}{C_o} \times \left[ \frac{V}{m} \right] \quad (2)$$

## Batch elution procedures

Different eluting agents were studied for uranium recovery from loaded adsorbents. In each experiment, 0.05 g of loaded adsorbent was shaken with 25 mL of eluting agent of different concentrations for 30 min at 25 °C.

## Uranium (VI) precipitation

The eluted solution was subjected to precipitation by adding 40% NaOH solution till reaching pH 7. Uranium was then precipitated as sodium diuranate (Na<sub>2</sub>U<sub>2</sub>O<sub>7</sub>).

**Table 2** Chemical composition of major oxide (wt %)

Oxide	SiO <sub>2</sub>	Al <sub>2</sub> O <sub>3</sub>	Fe <sub>2</sub> O <sub>3</sub> <sup>T</sup>	CaO	MgO	P <sub>2</sub> O <sub>5</sub>	Na <sub>2</sub> O	K <sub>2</sub> O	MnO	TiO <sub>2</sub>	L.O.I.
Wt, %	71.5	10.30	2.61	4.50	2.0	0.31	2.32	3.67	0.07	0.60	1.90

**Table 3** Trace elements content (mg/kg) using ICP-OES technique

Element	Ba	Mo	Ni	Zr	Pb	Rb	Sr	Cu	Y	Zn	Nb	U
Conc. (mg/Kg)	342	223	35	180	100	380	30	50	60	250	40	1400

**Table 4** Chemical analyses of Gattar leach liquor

Ions	Si	Al	Fe	Ca	Mg	P	Na	K	Ti	Mn	
Conc. (g/L)	2.22	2.72	0.913	1.6	0.60	0.135	1.72	3.55	0.12	0.03	
Ions	Mo	Ba	Zr	Ni	Pb	Rb	Sr	Cu	Y	Zn	U
Conc. (g/L)	0.06	0.09	0.05	0.009	0.026	0.101	0.008	0.013	0.016	0.07	0.443

## Analytical procedures

Uranium (VI) was analyzed in solution by UV spectrometer using Arsenazo III as indicator at 650 nm [28]. Results were confirmed by modified Davies and Grey oxidometric titration against ammonium meta-vanadate [29, 30].

## Results and discussion

### Effect of initial uranium concentration

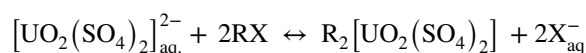
Uranium adsorption efficiency was found to be constant from 50 to 150 mg/L; (Fig. 1). It is obvious that at low uranium concentrations, the available uranyl ions are less than the number of active sites on the surface of the adsorbent. The adsorption efficiency decreased beyond 150 mg/L due to the gradual saturation of active sites. As for QSLC, uranium adsorption remained constant till 450 mg/L and then decreased gradually.

The maximum value of uranium uptake for AL was 69 mg/g at conc. 150 mg/L of U, while the maximum uptake for QSLC was 207 mg/g at conc. 450 mg/L of U (VI).

### Effect of pH

The pH of the aqueous solution can influence the aqueous chemistry of uranium [31]. The mobility of present ions in the medium is affected by concentration of  $H^+$  ions. Moreover, it also affects interest and capacity of adsorbents for target species. There is always a competition between  $H^+$  ions and other ionic species in the medium. If there are polyanionic or polycationic species in solution, interactions are fairly affected by the pH of the medium.

The effect of initial solution pH was investigated by preparing a series solution having a different pH within the range 0.5 to 6, adjusted by using either 0.5 M  $H_2SO_4$  and 0.5 M NaOH. 0.05 g of each adsorbent were allowed to contact with 25 mL of aqueous solution of U (VI) concentration 150 mg/L with AL and 450 mg/L with QSLC at 25 °C. Results shown in (Fig. 2a) clarifies that uranium uptake increases from pH 1 to 2.5 (69 mg/g for AL and 207 mg/g for QSLC). Beyond pH 2.5, the adsorption efficiency starts decreasing with pH elevation. The optimum pH for adsorption is 2.5. Bivalent  $[UO_2(SO_4)_2]^{2-}$  anionic species and neutral uranium sulfate complex  $[UO_2SO_4]$  were found to be dominant lower pH using Hydra-Medusa software as shown in Fig. 2b. Uranium anionic complexes are adsorbed on the resin and their interaction may be represented as follows;



where R represents the ion-exchange sites on the resin, and  $X^-$  for exchangeable chloride ions.

### Effect of contact time

The effect of contacting time was investigated through 5–60 min, (Fig. 3). 0.05 g of each adsorbent was mixed with 25 mL of uranium solution at pH 2.5. From the obtained results, uranium uptake increases with increasing contact time for the first 30 min (69 mg/g for AL and 207 mg/g for QSLC), thereafter remaining almost constant.

A contact time of 30 min. was found sufficient to establish equilibrium and used in all subsequent studies.

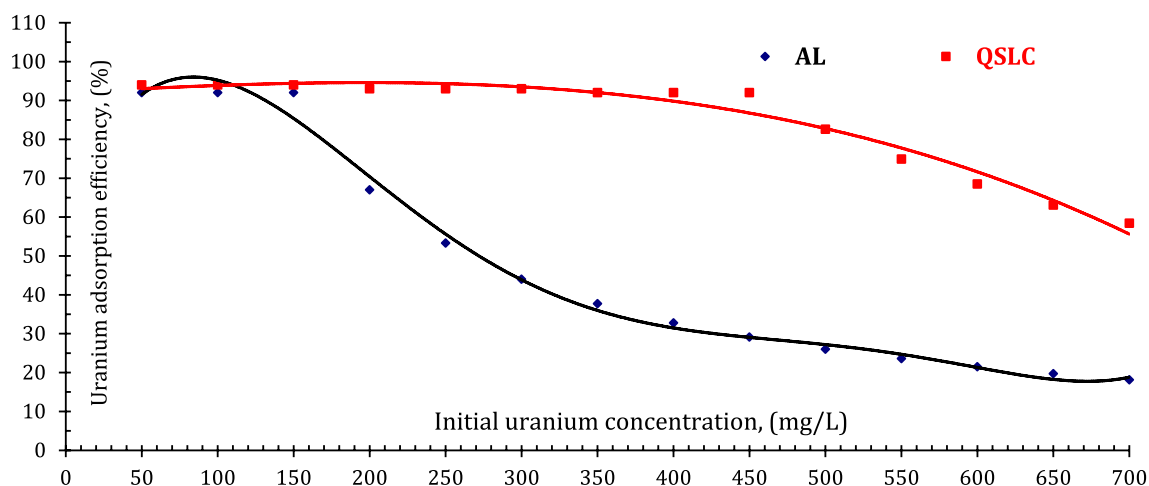


**Fig. 1** Effect of initial uranium concentration on U(VI) adsorption efficiency by AL & QSLC Adsorption conditions pH: 2.5, adsorbent dose: 0.05 g, Volume: 25 mL, 25 °C, Time: 30 min

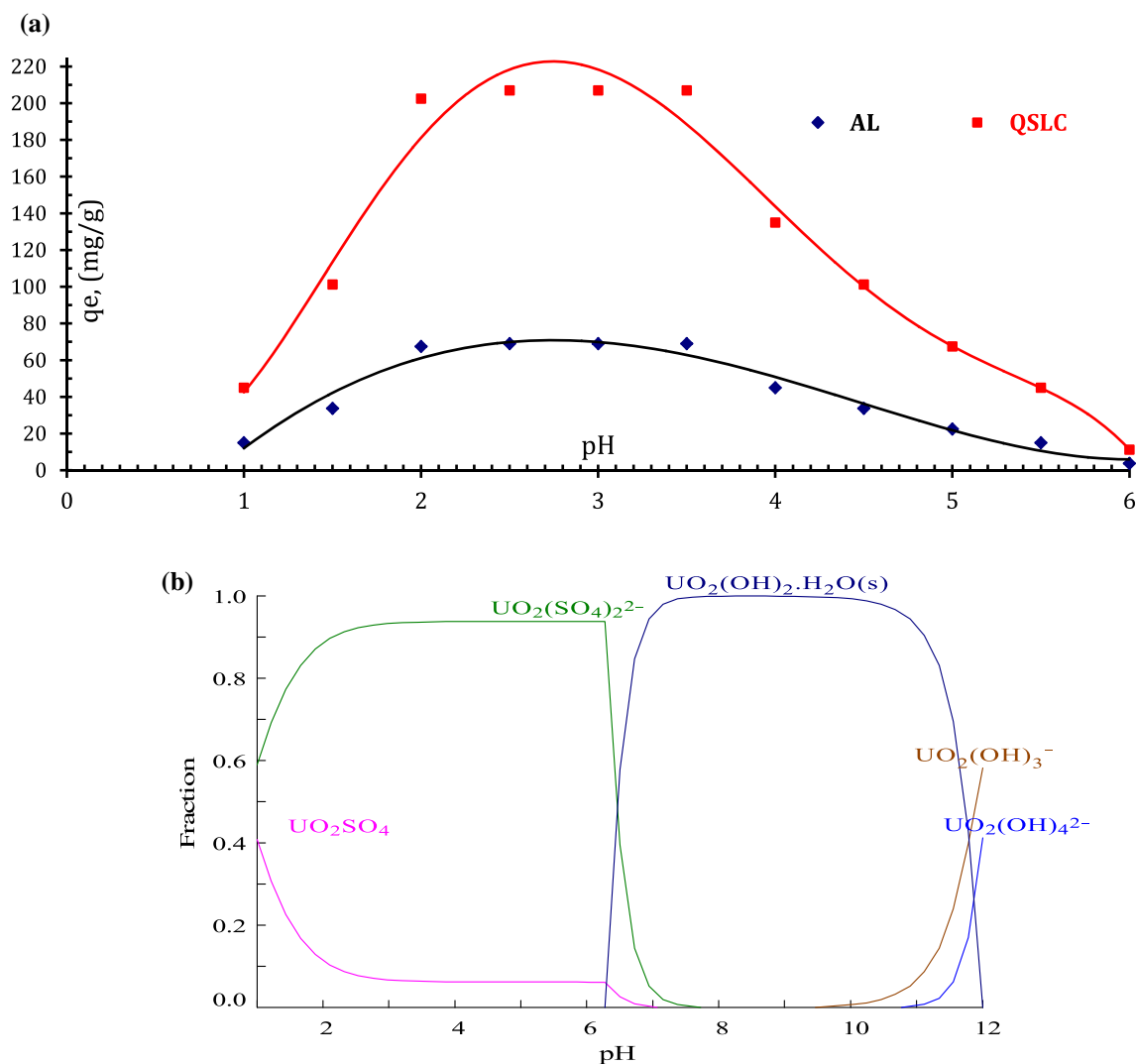


**Fig. 2 a** Effect of pH on uranium uptake by AL & QSLC. Adsorption conditions Uranium conc. 150 mg/L with AL and 450 mg/L with QSLC, adsorbent dose: 0.05 g, Vol.: 25 mL, 25 °C, Time: 30 min.

**b** Predicted aqueous speciation of uranium as a function of pH in  $H_2SO_4$  medium by Hydra-MEDUSA software

### Adsorption kinetic modeling

Kinetic parameters are helpful for the prediction of adsorption rate. The mechanism of uranium adsorption by both adsorbents was investigated according to pseudo-first order and pseudo-second order models [32–34]. The pseudo-first order kinetic model is represented by the following equation:

$$\text{Log}(q_e - q_t) = \text{Log}q_e - \left( \frac{K_1}{2.303} \right) \cdot t \quad (3)$$

where  $K_1$  is the rate constant,  $q_e$  is the amount of metal adsorbed per unit mass at equilibrium and  $q_t$  is the amount adsorbed per unit time. Plotting  $\log(q_e - q_t)$  versus  $t$  gives a straight line as shown in (Fig. 4), which provide  $K_1$  and

$q_e$  from its slope and intercept, respectively. The plot diagram suggested the applicability of the pseudo-first order kinetic model to fit the practical data as given in (Table 5). The calculated value of  $q_e$  was found 123.73 mg/g for AL and 346.57 mg/g for QSLC, which is far from the experimental uptake capacity (69 mg/g for AL and 207 mg/g for QSLC). The experimental data did not agree with the first order kinetic model which is not suitable for explaining the studied system.

The pseudo-second order kinetic model is represented by the following equation:

$$\frac{t}{q_t} = \frac{1}{k_2 q_e^2} + \left( \frac{1}{q_e} \right) \cdot t \quad (4)$$

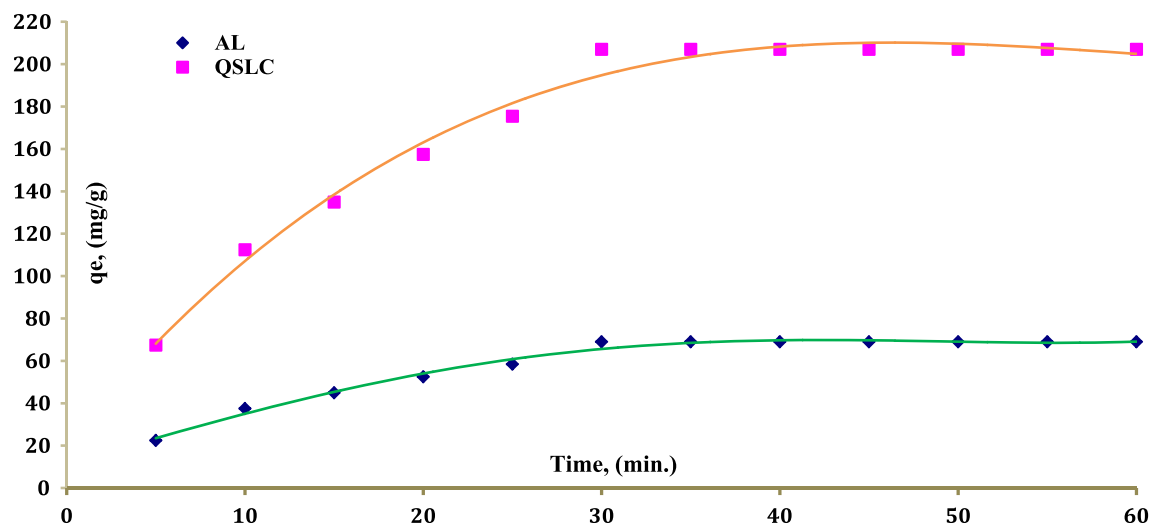


**Fig. 3** Effect of contact time on uranium uptake by AL & QSLC. Adsorption conditions Uranium conc. 150 mg/L mixed with AL, Uranium conc. 450 mg/L mixed with QSLC, pH: 2.5, adsorbent dose: 0.05 g, Vol.: 25 mL, temperature: 25 °C

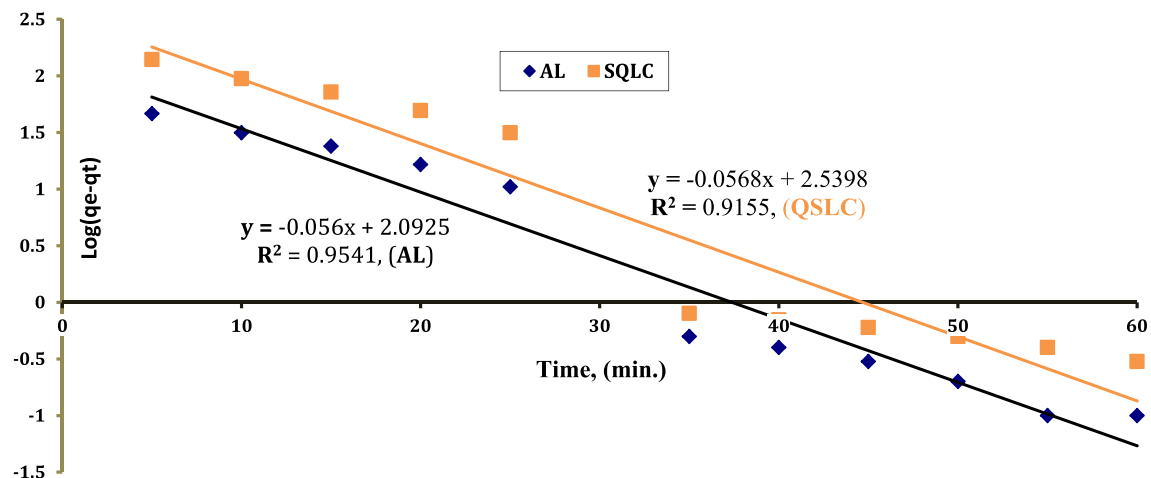


**Fig. 4** Pseudo-first order model of uranium adsorption onto AL & QSLC. Adsorption conditions Uranium conc. 150 mg/L mixed with AL, Uranium conc. 450 mg/L mixed with QSLC, pH: 2.5, adsorbent dose: 0.05 g, Volume: 25 mL, temperature: room temp., Time: 30 min

**Table 5** Kinetic parameters of uranium adsorption onto AL & QSLC

Adsorbents	Exp. capacity (qe, mg/g)	Pseudo-first order			Pseudo-second order		
		qe	K <sub>1</sub>	R <sup>2</sup>	qe	K <sub>2</sub>	R <sup>2</sup>
AL	69	123.73	0.1289	0.9541	69.44	0.00147	0.9949
QSLC	207	346.57	0.1308	0.9155	217.39	0.000452	0.9945

where  $K_2$  is the rate constant. The straight line of plot  $t/q_t$  versus  $t$  whose slope =  $1/q_e$  and the intercept =  $1/k_2 \cdot q_e^2$ . Figure 5, suggested the applicability of pseudo-second order kinetic model to fit the experimental data as shown in (Table 5). The calculated value of  $q_e$  was found to be 69.44 mg/g for AL and 217.39 mg/g for QSLC. The

calculated values according to second order kinetic model are in agreement with experimental data and therefore it is suitable for describing the studied system.

**Adsorption isotherm modeling**

The Langmuir model is based on the assumption that maximum adsorption occurs as saturated monolayer of adsorbate molecules on the adsorbent surface and that the energy of adsorption is constant, with no trans-migration of adsorbate on the surface of adsorbent [35]. Langmuir isotherm model is represented by the following equation:

$$\frac{C_e}{q_e} = \frac{1}{q_o b} + \frac{C_e}{q_o} \tag{6}$$

where  $C_e$  is the concentration at equilibrium,  $q_e$  is the amount of uranium adsorbed at equilibrium;  $q_o$  and  $b$  are Langmuir constants related to maximum uptake capacity and adsorption energy. The linear plot of  $C_e/q_e$  versus  $C_e$  shown in (Fig. 6) and (Table 6) clarifies that the adsorption process

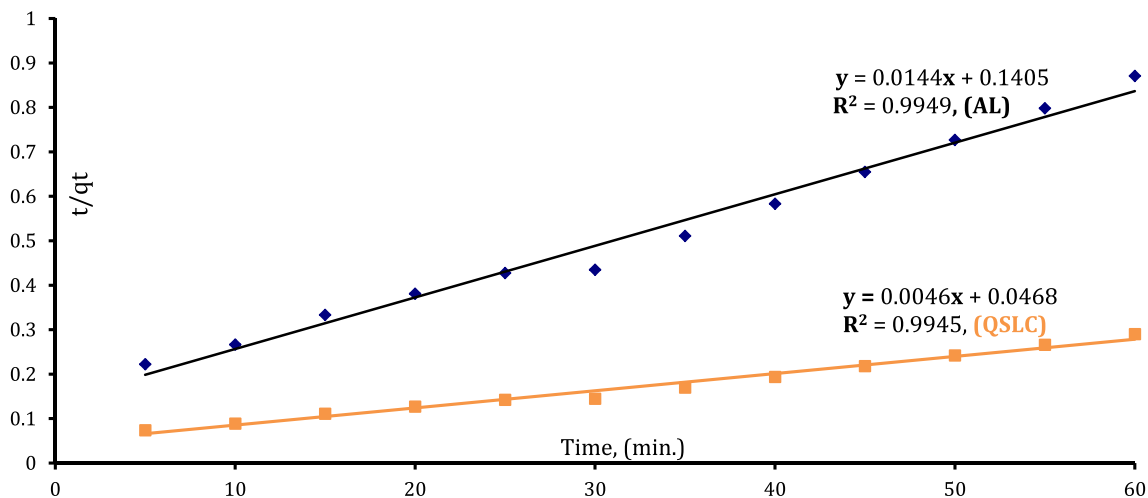


**Fig. 5** Pseudo-second order model of uranium adsorption onto AL & QSLC. Adsorption conditions Uranium conc. 150 mg/L mixed with AL, Uranium conc. 450 mg/L mixed with QSLC, pH: 2.5, adsorbent dose: 0.05 g, Volume: 25 mL, temperature: room temp., Time: 30 min

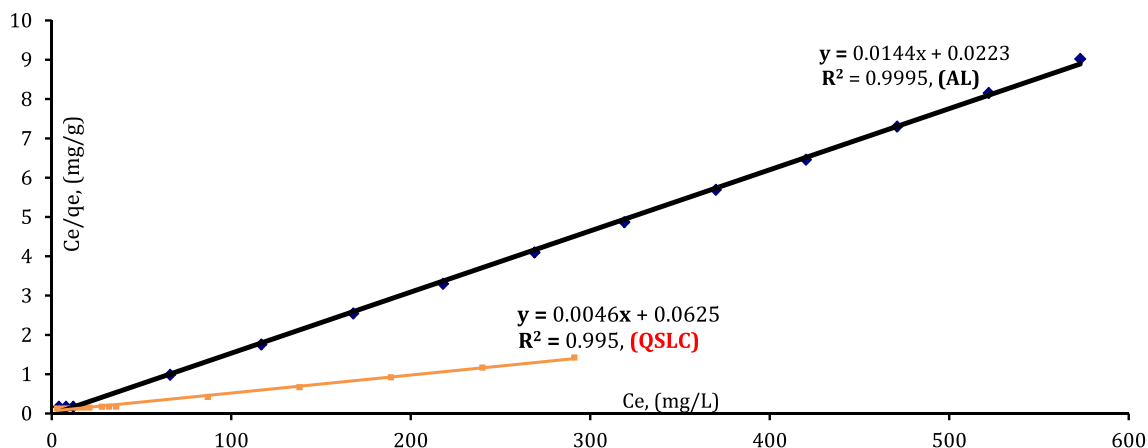


**Fig. 6** Langmuir isotherm model of uranium adsorption onto AL & QSLC. Adsorption conditions Uranium conc. 150 mg/L mixed with AL, Uranium conc. 450 mg/L mixed with QSLC, pH: 2.5, adsorbent dose: 0.05 g, Volume: 25 mL, temperature: room temp., Time: 30 min

**Table 6** Adsorption isotherm parameters of uranium adsorption onto AL & QSLC

Adsorbents	Exp. capacity $q_e$ , mg/g	Langmuir			Freundlich		
		$q_e$	$b$	$R^2$	$q_e$	$n$	$R^2$
AL	69	69.44	0.645	0.9995	33.24	8.32	0.477
QSLC	207	217.39	0.0327	0.995	29.55	2.45	0.7476



obeys Langmuir model. The correlation coefficient for the linear regression  $R^2=0.9995$  for AL and  $0.995$  for QSLC. The slope and intercept of the straight line were used to determine  $q_o$  and  $b$  as (69.44 mg/g and 0.645 g/mg) for AL and (217.39 mg/g and 0.0327 g/mg) for QSLC, respectively. Langmuir isotherm can be expressed in term of a dimensionless constant (separation factor),  $R_L$ ; which is defined by the equation:

$$R_L = \frac{1}{1 + bC_o} \quad (7)$$

where  $b$  is the Langmuir constant and  $C_o$  is the initial uranium concentration. If the values of  $R_L < 1$ , this indicates a favorable adsorption process, (Table 7).

The Freundlich isotherm model was applied to the adsorption as a means of data interpretation [36]. The Freundlich isotherm model is represented by the equation:

$$\text{Log}q_e = \text{Log}K_f + \left(\frac{1}{n}\right)\text{Log}C_e \quad (8)$$

where  $C_e$  is the concentration at equilibrium,  $q_e$  is the amount of uranium adsorbed at equilibrium;  $K_f$  and  $n$  are Freundlich constants corresponding to the adsorption uptake capacity and adsorption intensity, respectively. A plot of  $\text{Log}q_e$  versus  $\text{Log}C_e$  is shown in (Fig. 7).

The constants  $K_f$  and  $n$  were found to be (33.24 mg/g, 8.32 for AL), and (29.55 mg/g, 2.45 for QSLC), respectively.

The correlation coefficient  $R^2=0.477$  for AL and  $0.7476$  for QSLC, indicating that experimental data are better represented by Langmuir model rather than by Freundlich model (Table 6).

### Effect of adsorbent dose

The effect of adsorbent dose in the range of 0.01–0.1 g was studied. Results presented on Fig. 8 show that uranium uptake increases with increasing adsorbent dose till 0.05 g then starts to decrease for both AL and QSLC. The most convenient dose was chosen as 0.05 g. At low adsorbent doses, all the active sites are entirely exposed and adsorption is encouraged till all the surface of adsorbent becomes saturated. At higher adsorbent doses, the available uranium species in bulk are not sufficient enough to fulfill the entire adsorbent empty sites [37–39]. The maximum uptake capacities were 69 mg/g for AL and 207 mg/g for QSLC.

Furthermore, at high adsorbent doses, the available uranium ions in solution are not

### Effect of temperature

The effect of temperature on uranium uptake was studied using 0.05 g of each of the 2 adsorbents contacted with 25 mL of uranium solution of conc. 150 mg/L for AL and 450 mg/L for QSLC at pH 2.5 for 30 min. at temperature range 25–70 °C. Results shown in (Fig. 9) illustrate that

**Table 7** Calculated values of  $R_L$  for Langmuir model for AL & QSLC

U (mg/L)	50	100	150	200	250	300	350	400	450	500	550	600	650	700
RL, AL	0.030	0.015	0.010	0.007	0.006	0.005	0.004	0.003	0.003	0.003	0.002	0.002	0.002	0.002
RL, QSLC	0.379	0.234	0.169	0.132	0.109	0.093	0.080	0.071	0.064	0.058	0.053	0.048	0.045	0.042

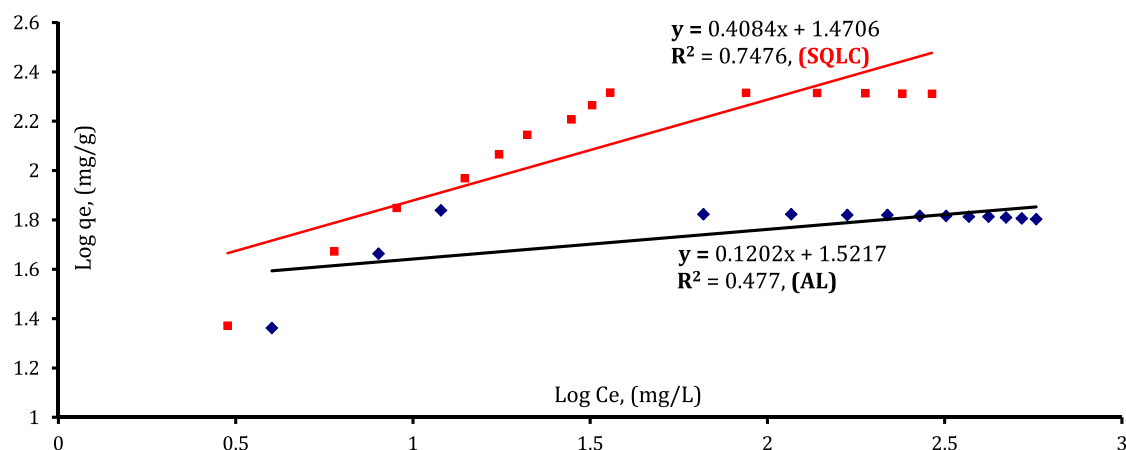


**Fig. 7** Freundlich isotherm model of uranium (VI) adsorption onto AL and QSLC. Adsorption conditions Uranium conc. 150 mg/L mixed with AL, Uranium conc. 450 mg/L mixed with QSLC, pH: 2.5, adsorbent dose: 0.05 g, Volume: 25 mL, temperature: room temp., Time: 30 min



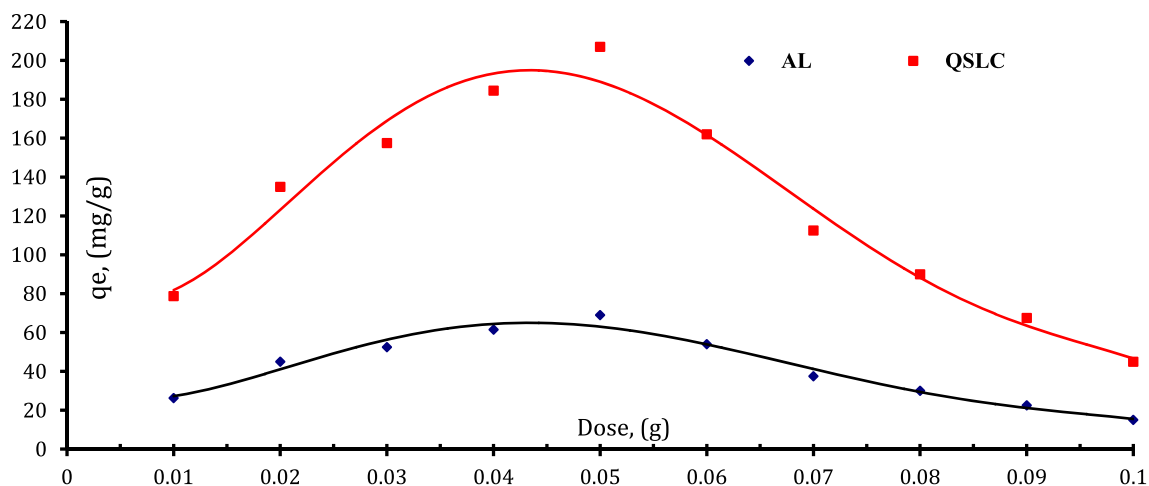


**Fig. 8** Effect of AL and QSLC dose on uranium uptake capacity. Conditions Uranium conc. 150 mg/L with AL & 450 mg/L with QSLC, pH: 2.5, Vol.: 25 mL, 25 °C, 30 min

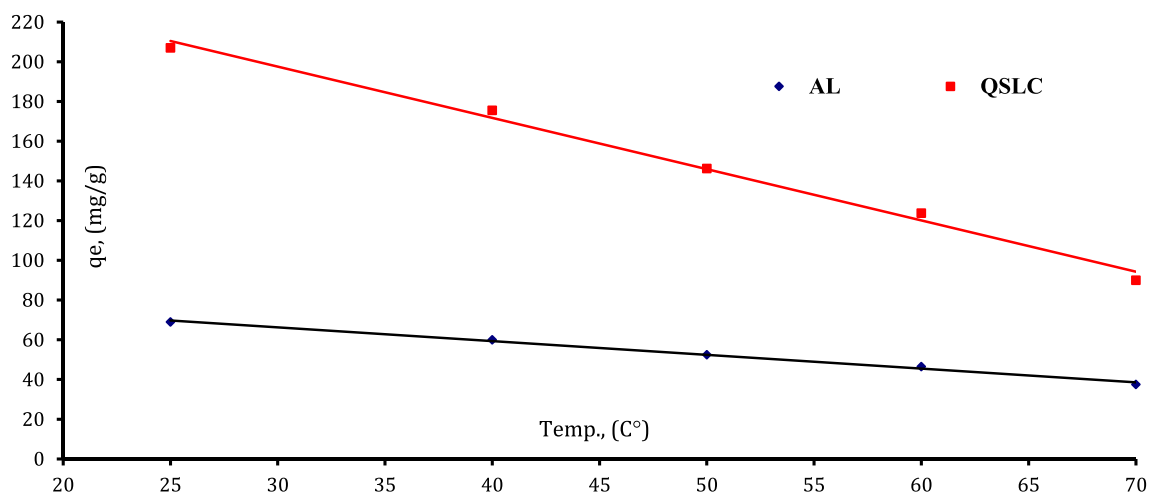


**Fig. 9** Effect of temperatures on uranium uptake capacity for AL and QSLC. Adsorption conditions Uranium conc., 150 mg/L mixed with AL, Uranium conc. 450 mg/L mixed with QSLC, pH: 2.5, Volume: 25 mL, adsorbent dose: 0.05 g, temperature: room temp., Time: 30 min

uranium uptake decreased linearly from 69 to 37.5 mg/g for AL and from 207 to 90 mg/g for QSLC with increasing temperature from 25 to 70 °C. Such behavior is due to the exothermic nature of uranium uptake process. The most suitable temperature that corresponds to the most efficient uranium adsorption was considered as the room temperature.

#### Thermodynamic studies of uranium adsorption

Thermodynamic parameters are calculated from the following equations [40]:

$$\Delta G = -2.303RT \cdot \text{Log}K_d \quad (9)$$

$$\Delta G = \Delta H - T\Delta S \quad (10)$$

$$\text{Log}K_d = \frac{\Delta S}{2.303R} - \frac{\Delta H}{2.303RT} \quad (11)$$

where  $\Delta G$  is the Gibbs free energy,  $\Delta H$  is the enthalpy change and  $\Delta S$  is the change in entropy.  $R$  is the universal gas constant ( $8.314 \text{ mol}^{-1} \text{ k}^{-1}$ ) and  $T$  is temp. in °K. The values of ( $\Delta H$ , KJ/mol) and ( $\Delta S$ , KJ/mol  $\text{K}^{-1}$ ) were calculated from the slope and intercept of the plot of  $\text{Log} K_d$  versus  $1/T$ , giving a slope of 2.3677 and intercept  $-7.2229$  for AL and a slope of 2.7606 and intercept of  $-8.5368$  for QSLC, (Fig. 10).

The results mentioned in (Table 8) indicate positive value of  $\Delta H$ , confirm that uranyl ions adsorption onto AL

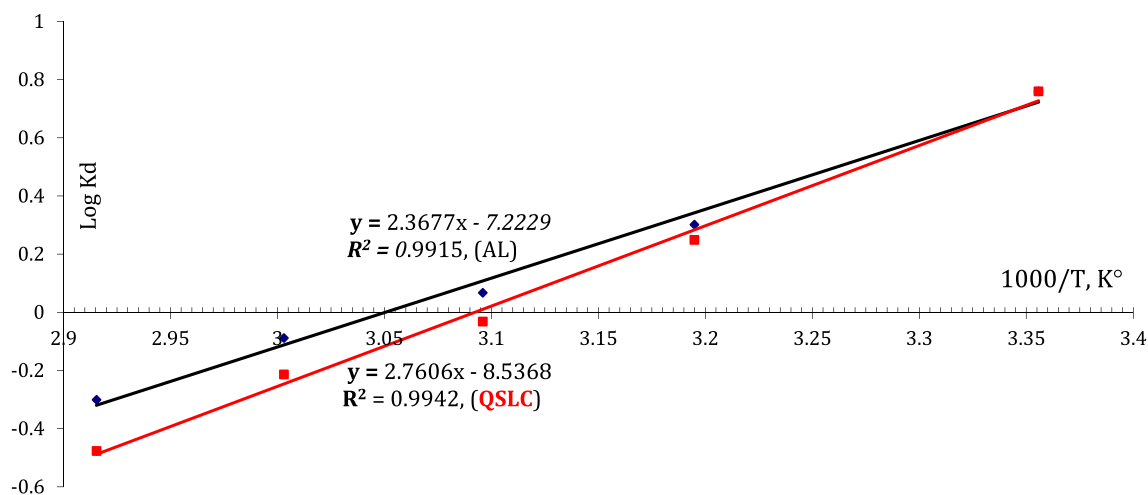


**Fig. 10** Log  $K_d$  versus  $1000/T$  for uranium adsorption onto AL and QSLC

**Table 8** Thermodynamic parameters of uranium adsorption onto AL & QSLC

Adsorbent (KJ/mol K <sup>-1</sup> )	$\Delta H$ (KJ/mol)	$\Delta S$ (KJ/mol K <sup>-1</sup> )	$\Delta G$ (KJ/mol)				
			298 °K	313 °K	323 °K	333 °K	343 °K
AL	-45.33	-0.1375	-4.334	-1.8040	-0.4140	0.5637	1.977
QSLC	-52.85	-0.1628	-4.334	-1.490	0.1990	1.3636	3.133

or QSLC is an exothermic process. The negative value of  $\Delta S$ , indicate decrease in the randomness of the adsorption process in the investigated system with change in the hydration of the adsorbed uranyl ions. The increase values of  $\Delta G$ , showed that the adsorption process is spontaneous. The increase in  $\Delta G$  values from 25 to 70 °C, with increasing temperature showed that the adsorption is unfavorable at high temperatures.

### Effect of interfering ions

The tested of interfering elements were chosen as they persist within the matrix of the studied leach liquor. The effect of interfering elements were separately studied by introducing each one in 25 mL of uranium solution containing 150 mg/L or 450 mg/L mixing with 0.05 g of each adsorbent AL or QSLC under optimum adsorption conditions. Obtained results shown in (Table 9).

The interfering elements can cause a decline in uranium adsorption that does not exceed 2%. The coexistence of such elements does not interfere with the adsorption process and it proves it possible to be applied successfully to extract uranium from the studied geologic sample.

### Uranium (VI) elution

Desorption is an economically important parameter in adsorption processes [41]. Three mineral acids ( $H_2SO_4$ ,

**Table 9** Effect of interfering elements on uranium adsorption (%) by AL & QSLC

Elements	Conc. (mg/L)	Adsorption (%)	Elements	Conc. (mg/L)	Adsorption (%)
K	4000	92	Rb	100	90
Si	3000	92	Ba	100	92
Al	3000	92	Mo	100	92
Na	2000	92	Zn	100	92
Ca	2000	92	Ni	50	91
Mg	1000	91	Zr	50	90
Fe	1000	91	Sr	50	92
P	500	91	Cu	50	92
Ti	500	91	Y <sup>3</sup>	50	92
Mn	500	91	Pb	50	92

Adsorption conditions Uranium conc., 150 mg/L mixed with AL, Uranium conc. 450 mg/L mixed with QSLC, pH: 2.5, Vol. 25 mL, adsorbent dose: 0.05 g, 25°C, Time: 30 min

$HCl$  and  $HNO_3$ ) with different concentrations 0.1–1 M were tested. A volume of 25 mL of acid solution was allowed to elute uranium from 0.05 g loaded adsorbent for 20 min. Results in (Table 10) show that uranium elution efficiency increased by increasing acid concentration. 0.25 M  $H_2SO_4$  solution was chosen to be the most convenient eluting agent due to its cheapness.

**Table 10** Effect of eluting agent's conc. on uranium elution efficiency from loaded AL & QSLC

Concentration (M)	Elution efficiency (%)		
	H <sub>2</sub> SO <sub>4</sub>	HCl	HNO <sub>3</sub> /NO <sub>3</sub>
0.10	78	60	76
0.25	92	70	84
0.50	92	81	92
0.75	92	82	92
1.00	92	85	92

Adsorption conditions Uranium conc., 150 mg/L mixed with AL, Uranium conc. 450 mg/L mixed with QSLC, pH: 2.5, Vol. 25 mL, adsorbent dose: 0.05 g, 25°C, Time: 30 min

## Characterization of AL and QSLC adsorbents

### Fourier transform infrared spectrometer characterization

FTIR spectra are useful in identifying molecular functional groups [42]. Thermo Scientific Nicolet IS10 FTIR instrument was used in a range 400–4000 cm<sup>-1</sup>. The FTIR spectra of AL and QSLC before and after uranium adsorption are given in (Fig. 11).

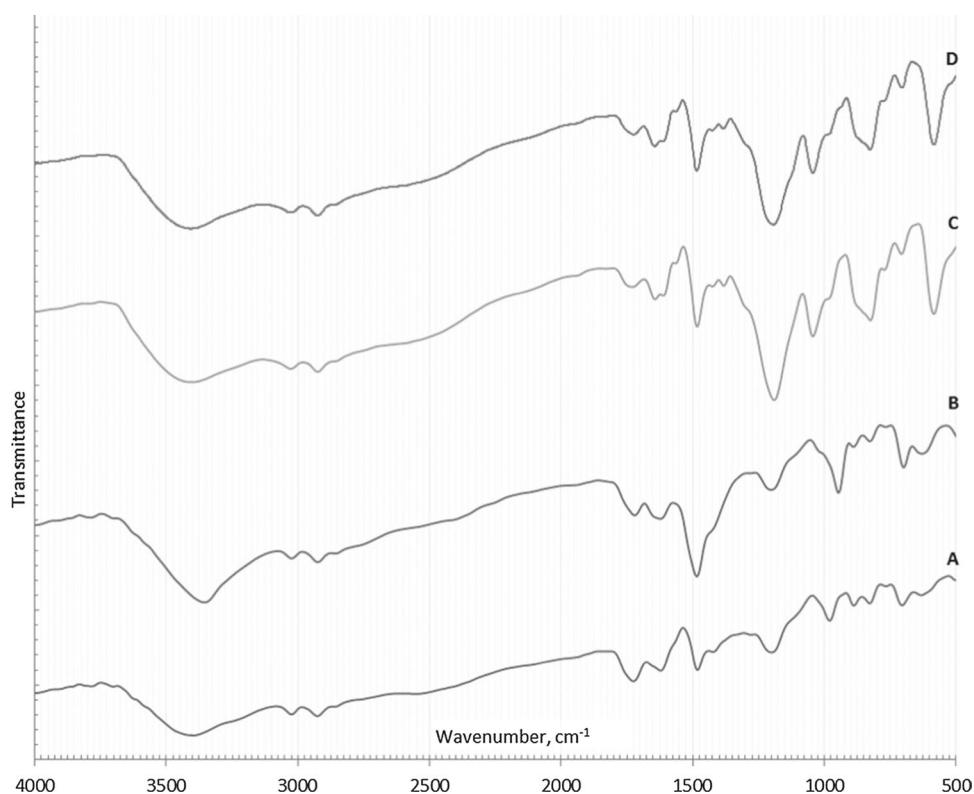
The bands appeared at 3780.04 and 3699.33 cm<sup>-1</sup> are attributed to OH stretching vibration of water adsorbed. Band found at 3400.21 cm<sup>-1</sup> is related to OH stretching in carboxylic [43, 44]. The peak at 3023 cm<sup>-1</sup> is related to

Ar–H stretching. The C–H stretching in alkanes is obtained at 2925.02 cm<sup>-1</sup>. One band at 1724.98 cm<sup>-1</sup> is related to monomer C=O in carboxylic. The peak at 1620.12 cm<sup>-1</sup> is related to NH<sub>2</sub> in plane bending (–NH<sub>3</sub><sup>+</sup>). The bands at 1481.92 and 1418.64 cm<sup>-1</sup> are attributed to Aromatic C=C in ring stretching [45, 46]. The peak at 1278.16 cm<sup>-1</sup> is related to Ar–N stretching.

The C–N stretching in amine is obtained at 1198.15 cm<sup>-1</sup>. The peak at 979.27 cm<sup>-1</sup> is related to N–O. The band at 888.28 cm<sup>-1</sup> is related to =C–H alkenes out of plane. While, 825.91 cm<sup>-1</sup> is attributed to aromatic C–H out of plane. On the other hands, two bands at 762.88 and 705.50 cm<sup>-1</sup> are obtained due to N–H wag amines (broad) bands. While, 631.92 and 499.36 cm<sup>-1</sup> are related to N–H oscillation (–NH<sub>3</sub><sup>+</sup>), (Fig. 11a). On the other hand, the major contributions of AL groups have been shifted or absence due to the adsorption of uranium (Fig. 11b).

The band at 3405.03 cm<sup>-1</sup> is related to monomer OH carboxylic. The peak at 3026.59 cm<sup>-1</sup> is related to broad (–NH<sub>3</sub><sup>+</sup>). Stretching band of alkane CH is related to 2924.78 cm<sup>-1</sup>. The peak observed at 1727.53 cm<sup>-1</sup> correspond to monomer C=O in carboxylic. The peak for C=N ring stretching in quinoline is observed at 1644.18 cm<sup>-1</sup>. Two peaks are observed at 1607.96 and 1563.39 cm<sup>-1</sup> for NH in plane bending (–NH<sub>3</sub><sup>+</sup>). The band of Ar C–C in ring stretching is obtained at 1483.72 cm<sup>-1</sup>. The peaks at 1321.32 and 1382.08 cm<sup>-1</sup> are related to S=O sulfate. While, 1190.72 cm<sup>-1</sup> is related to S=O sulphonyl chloride

**Fig. 11** FTIR of activated Lewatit **a**, activated Lewatit after adsorption of uranium **b**, quinoline Silicate Lewatit composite **c** and Quinoline Silicate Lewatit composite after uranium adsorption **d**



stretching band. One peak at  $1045.10\text{ cm}^{-1}$  is attributed to Si–OR (broad) band. On the other hand, the band of CH out of plane is obtained at  $823.44\text{ cm}^{-1}$ . The peak at  $823.72\text{ cm}^{-1}$  is attributed to aromatic C–H out of plane. One peak at  $771.35\text{ cm}^{-1}$  is related to alkyl halides stretching. While the band at  $707.54\text{ cm}^{-1}$  is related to S–OR. Two peaks are observed at  $584.13$  and  $467.93\text{ cm}^{-1}$  for N–H oscillation ( $-\text{NH}_3^+$ ), (Fig. 11c). On the other hand, the major contributions of QSLC groups have been shifted or absence due to the adsorption of uranium (Fig. 11d).

### Scanning electron microscope (SEM)

Activated Lewatit, AL before and after uranium adsorption were tested by SEM. It's obvious that AL with high effective surface area and high sorption capacity for uranium, as shown in (Fig. 12a, b). Quinoline Silicate Lewatit composite QSLC and after uranium adsorption were shown in (Fig. 12c, d).

### Energy-dispersive X-ray spectroscopy (EDX)

EDX was used to determine the elements present in 4 different samples mentioned in Fig. 13b.

### Elemental analysis (CHNS)

The CHNS elemental analysis of AL and QSLC were obtained (Table 11). The elemental analysis of QSLC showed an elevated C, H, and N content than the activated Lewatit. This confirms the successful incorporation of quinoline. The presence of S element (3.15%) in QSLC is due to the sulfuric acid washing step during the synthesis of the composite.

### X-ray Fluorescence (XRF)

The two adsorbents were identified by XRF after adsorption of uranium. Figure 14 involves the appearance of silica and sodium in the composite, supporting the fact that sodium metasilicate was successfully integrated into the surface of Lewatit. The composite shows much more affinity to uranium than AL.

### Uranium (VI) recovery from a geologic sample

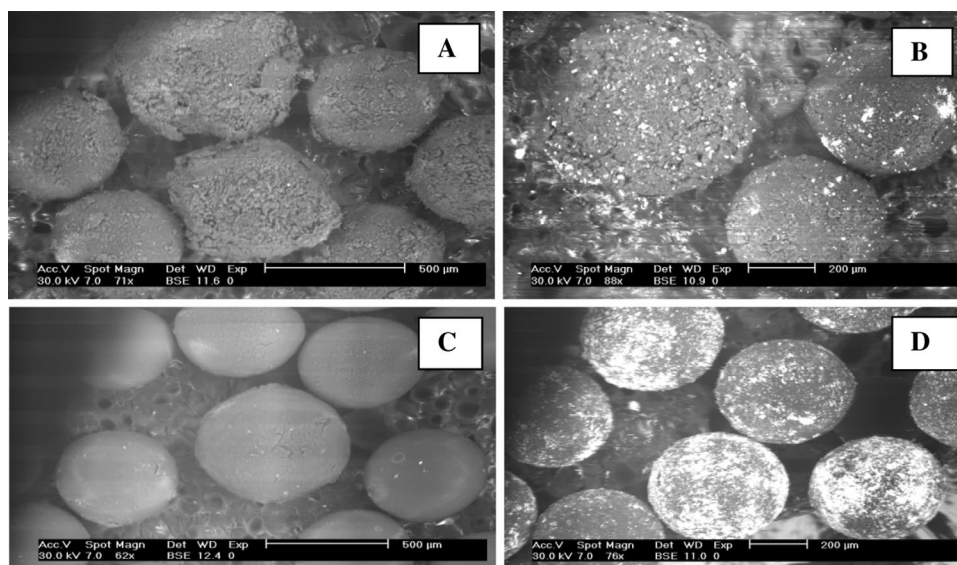
The applied experiments were carried out under optimum conditions by mixing 3 L of leach liquor solution of concentration  $443\text{ mg/L}$  of uranium with 2 g of QSLC and stirring 9L assaying  $147\text{ mg/L}$  of uranium with 2 g of AL at pH 2.5 for 30 min. The obtained results revealed that uranium adsorption efficiency was 92%. The uranium (VI) loaded on AL or QSLC was eluted by 500 mL of 0.25 M  $\text{H}_2\text{SO}_4$  solution. Eluted uranium was precipitated using 40% NaOH at pH 7 as sodium diuranate ( $\text{Na}_2\text{U}_2\text{O}_7$ ). The uranium concentrate was characterized by ICP-OES, XRF and EDX analysis techniques. Results are shown in (Table 12) and (Figs. 15, 16). Uranium content in the concentrate produced by AL & QSLC was 70% attaining a purity of 93.33% with a small amount of impurities.

A comparative study for uptake capacity (mg/g) of different adsorbents for uranium is shown in (Table 13).

### Conclusion

Both adsorbents were comparatively used for uranium (VI) adsorption from sulfate solution. The optimum conditions of batch technique: 3 Liters solution volume assaying

**Fig. 12** SEM of Activated Lewatit **a**, Activated Lewatit after uranium adsorption **b**, Quinoline Silicate Lewatit composite **c**, and Quinoline Silicate Lewatit composite after uranium adsorption **d**



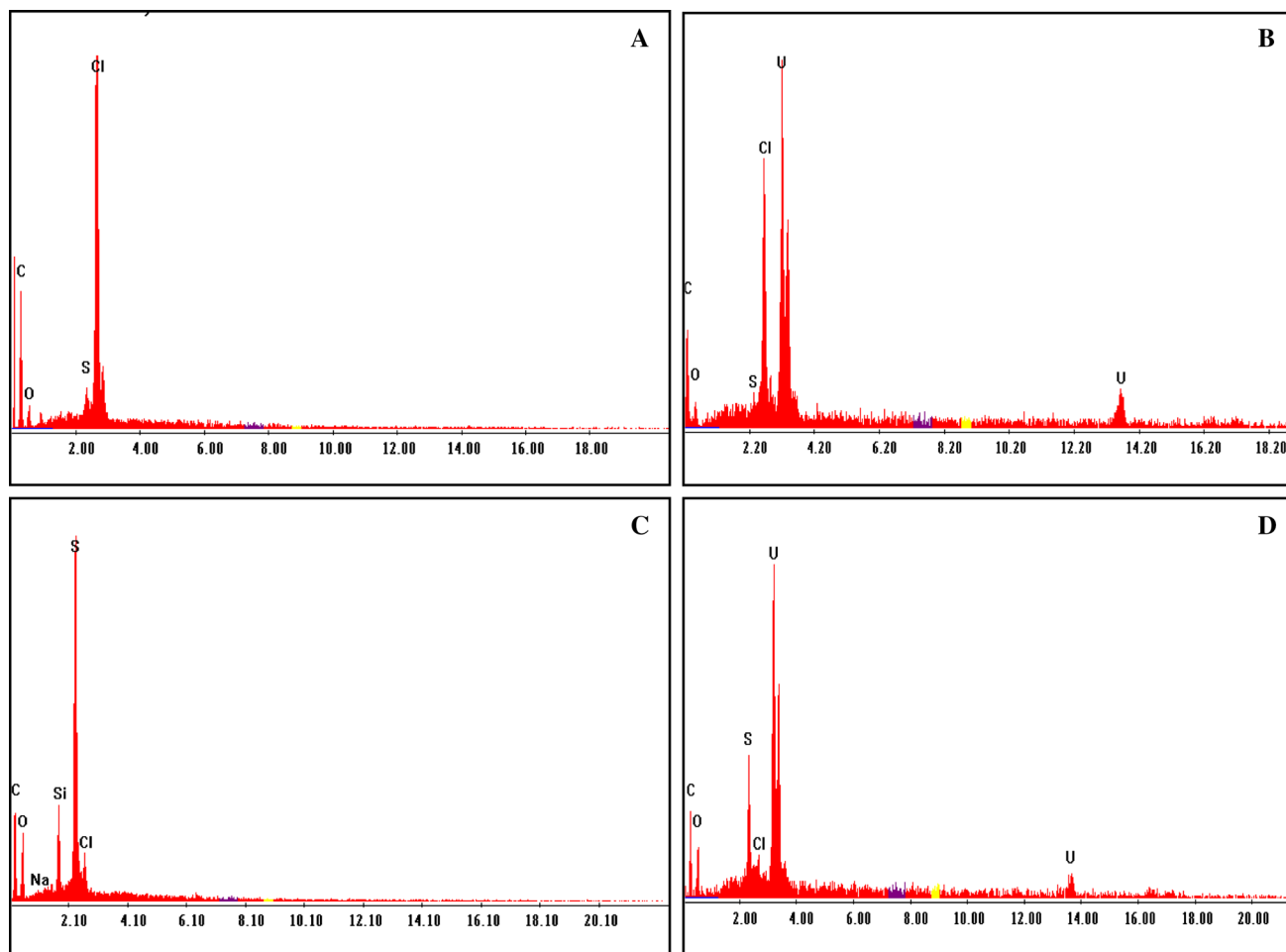


**Fig. 13** EDX of Activated Lewatit **a**, Activated Lewatit after uranium adsorption **b**, Quinoline Silicate Lewatit composite **c** and Quinoline Silicate Lewatit composite after uranium adsorption **d**

**Table 11** The CHNS elemental analysis of AL and QSLC

Adsorbent	C	H	N	S
Activated Lewatit AL	52.84	4.89	3.15	–
Quinoline Silicate Lewatit composite QSLC	69.37	5.74	3.20	3.15

443 mg/L U(VI) with 2 g of QSLC or 9 Liters assaying 147 mg/L U (VI) with 2 g of AL at pH 2.5 for 30 min. at room temperature. Under these conditions, the obtained maximum uptake capacities for each adsorbent AL and QSLC were 69.44 mg/g and 217.39 mg/g. The studied

thermodynamic parameters resulted in more negative values for  $\Delta H$  and  $\Delta S$  for QSLC indicating more exothermic process with a decrease in randomness of the system. Values of  $\Delta G$  indicate a spontaneous adsorption process. The obtained kinetic data fitted well with pseudo-second order kinetic model. Langmuir adsorption isotherm model was found more suitable for explaining the adsorption process. Uranium elution can be easily performed using 0.25 M  $H_2SO_4$  acid. The eluted uranium was precipitated using 40% NaOH as sodium diuranate ( $Na_2U_2O_7$ ). The final uranium concentrate from studied sample had a uranium content of 70% with a purity of 93.33% and acceptable level of impurities.

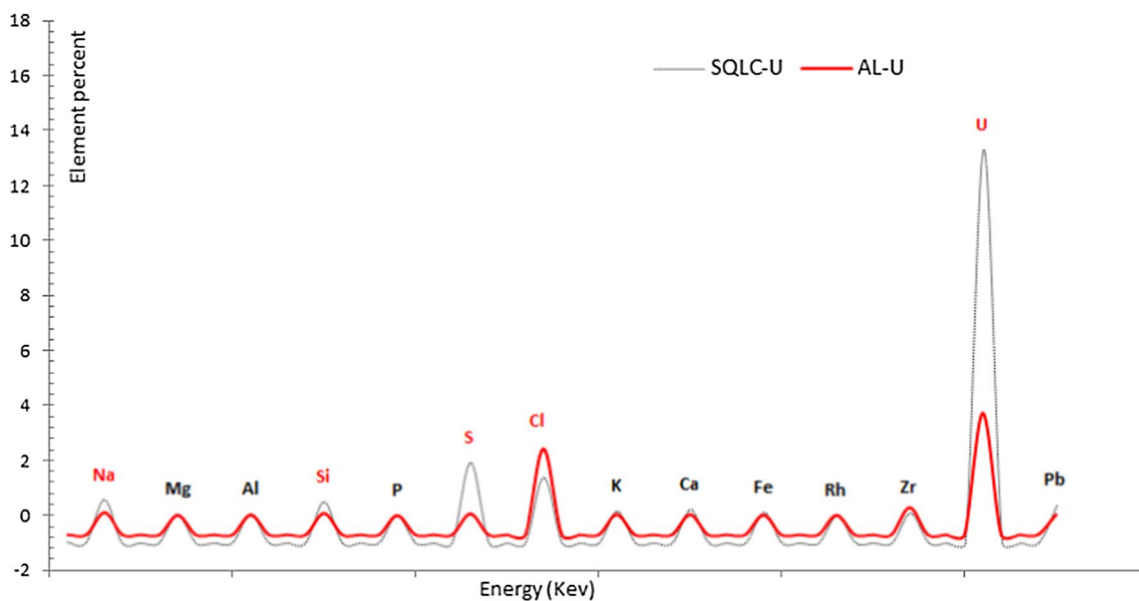


Fig. 14 XRF analysis of AL and QSLC after uranium adsorption

Table 12 ICP-OES specification of Gattar uranium concentrate produced by AL & QSLC

Element	U	Si	Al	Fe	Ca	Mg	Co	Ni	Cu
Content (%)	70.00	0.006	0.0121	0.0070	0.0290	0.0190	0.0012	0.0013	0.0038
Element	Cd	Cr	Na	K	Mn	V	Zn	Pb	Zr
Content (%)	0.0002	0.0013	5.017	0.0110	0.0006	0.0023	0.0011	0.0021	0.0031

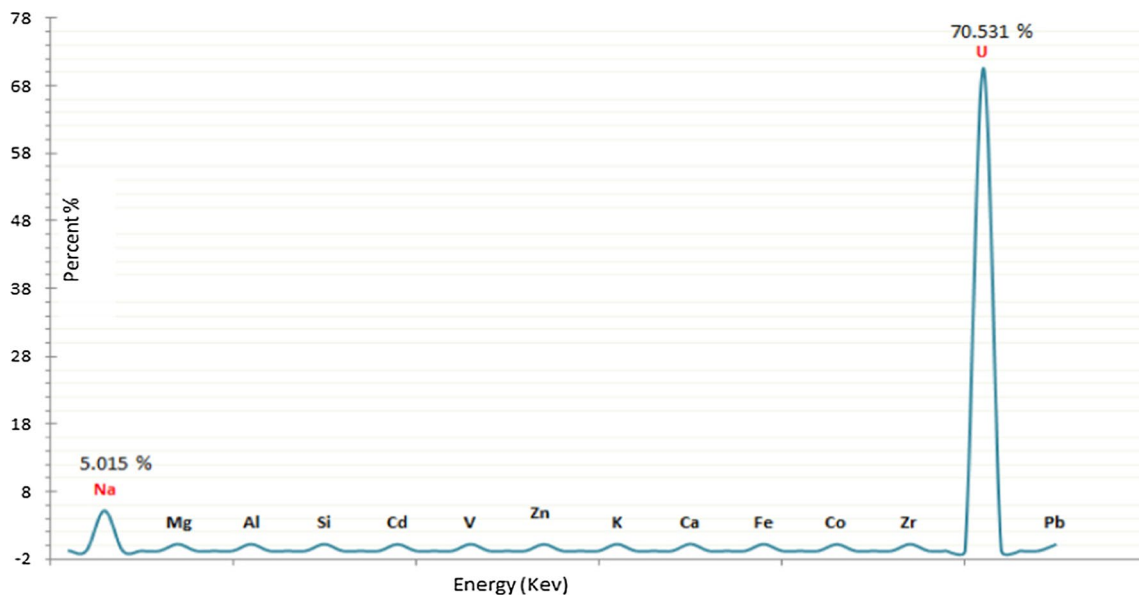


Fig. 15 XRF of the prepared Na<sub>2</sub>U<sub>2</sub>O<sub>7</sub> from Gattar sample

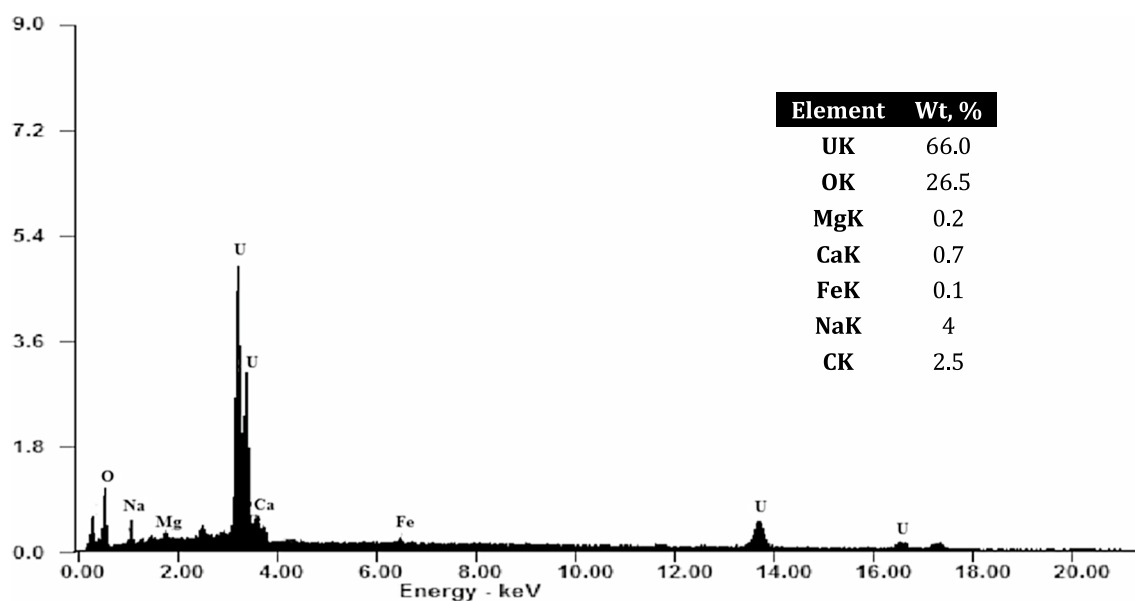


Fig. 16 EDX of the prepared  $\text{Na}_2\text{U}_2\text{O}_7$  from Gattar sample

**Table 13** Comparison of uranium adsorption capacity by different adsorbents

Adsorbent	Type	Qmax (mg/g)	Manufacturer	References
Ambersep 920 U ( $\text{SO}_4^{2-}$ )	SBA	58.82	Rohm & Haas Co., USA	[31]
Amberlite IRA-402	SBA	213	Rohm & Haas Co., USA	[47]
Amberlyst A27	SBA	131.57	Rohm & Haas Co., US.	[48]
Amberlite CG-400	SBA	112.36	Rohm & Haas Co., USA	[49]
Amberlite IRA-910U	SBA	108	Rohm & Haas Co., USA	[50]
Dowex A	SBA	79	Dow Chemical Co., USA	[50]
Dowex 21 K	SBA	57.63	Dow Chemical Co., USA	[51]
Dowex 1	SBA	84.87	Dow Chemical Co., USA	[51]
Dowex 2X8	SBA	71.2	Dow Chemical Co., USA	[52]
Ambersep 920 U ( $\text{Cl}^-$ )	SBA	50	Rohm & Haas Co., USA	[53]
Rossion-25A	SBA	61.7	Stans Energy Co., Russia	[54]
Purolite A500U	SBA	58.9	Purolite, Co., USA	[54]
Amberlite IRA 67	WBA	60	Rohm & Haas Co., USA	[9]
Lewatit TP 260	WAC	58.33	LANXESS-AG Co., Germany	[18]
Ambersep 400 ( $\text{SO}_4^{2-}$ )	SBA	50	Rohm & Haas Co., USA	[55]
Lewatit mono plus M500	SBA	40.65	LANXESS-AG Co., Germany	[15]
Tulsion CH-96	WAC	70	Thermax Chem. Co., India	[56]
Activated Lewatit mono plus M500	SBA	69.44	LANXESS-AG Co., Germany	Present work
Quinoline Silicate Lewatit composite	SBA	217.39	LANXESS-AG Co., Germany	Present work

SBA: strong base anion exchanger, WBA: weak base anion exchanger, WAC: weak acid cation exchanger

**Acknowledgements** This work was funded by the Nuclear Materials Authority as a part of its research activities. This article was reviewed and approved for publishing by the Nuclear Materials Authority with no obligation on the authors' part to revise the manuscript.

### Compliance with ethical standards

**Conflict of interest** The authors declare that they have no conflict of interests.



**Ethical approval** This article does not contain any studies with human participants or animals performed by any of the authors.

## References

- Dong W, Brooks SC (2008) Formation of aqueous  $\text{MgUO}_2(\text{CO}_3)_3^{2-}$  complex and uranium anion exchange mechanism onto an exchange resin. *Environ Sci Technol* 42:1979–1983. <https://doi.org/10.1021/es0711563>
- Shavinskii BM (2003) Anion-exchange recovery of thorium from uranium: analytical and preparation aspects. *Radiochemistry* 45:146–148. <https://doi.org/10.1023/A:1023877008197>
- Wen Z, Huang K, Niu Y et al (2020) Kinetic study of ultrasonic-assisted uranium adsorption by anion exchange resin. *Colloids Surf A* 585:124021. <https://doi.org/10.1016/j.colsurfa.2019.124021>
- Wódkiewicz L, Dybczyński R (1972) Effect of resin cross-linking on the anion-exchange separation of rare earth complexes with DCTA. *J Chromatogr A* 68:131–141. [https://doi.org/10.1016/S0021-9673\(00\)88770-1](https://doi.org/10.1016/S0021-9673(00)88770-1)
- Rychkov VN, Smirnov AL, Gortsunova KR (2014) Sorption of uranium from underground leaching solutions with highly basic anion exchangers. *Radiochemistry* 56:38–42. <https://doi.org/10.1134/S1066362214010081>
- Stoliker DL, Kaviani N, Kent DB, Davis JA (2013) Evaluating ion exchange resin efficiency and oxidative capacity for the separation of uranium(IV) and uranium(VI). *Geochem Trans* 14:1. <https://doi.org/10.1186/1467-4866-14-1>
- Riegel M, Tokmachev M, Hoell WH (2008) Kinetics of uranium sorption onto weakly basic anion exchangers. *React Funct Polym* 68:1072–1080. <https://doi.org/10.1016/j.reactfunctpolym.2008.02.009>
- Kowalczyk M, Hubicki Z, Kołodyńska D (2013) Removal of heavy metal ions in the presence of the biodegradable complexing agent of EDDS from waters. *Chem Eng J* 221:512–521. <https://doi.org/10.1016/j.cej.2013.02.010>
- Riegel M, Schlitt V (2017) Sorption dynamics of uranium onto anion exchangers. *Water* 9:268. <https://doi.org/10.3390/w9040268>
- Koodynska D, Hubicki Z (2012) Investigation of sorption and separation of lanthanides on the ion exchangers of various types. In: Kilislioglu A (ed) *Ion exchange technologies*. InTech
- Pehlivan E, Cetin S (2009) Sorption of Cr(VI) ions on two Lewatit-anion exchange resins and their quantitative determination using UV–visible spectrophotometer. *J Hazard Mater* 163:448–453. <https://doi.org/10.1016/j.jhazmat.2008.06.115>
- Galán B, Calzada M, Ortiz I (2006) Separation and Concentration of Cr(VI) from ground waters by anion exchange using lewatic MP-64: mathematical modelling at acidic pH. *Solv Extr Ion Exchange* 24:621–637. <https://doi.org/10.1080/07366290600762413>
- Purkayastha D, Mishra U, Biswas S (2014) A comprehensive review on Cd(II) removal from aqueous solution. *J Water Process Eng* 2:105–128. <https://doi.org/10.1016/j.jwpe.2014.05.009>
- Khawassek Y (2017) Anion exchange of uranium from sulfuric acid solution: adsorption and kinetics characteristics. In: ALTA 2017 URANIUM-REE SESSIONS. [https://www.researchgate.net/publication/328062508\\_ANION\\_EXCHANGE\\_OF\\_URANIUM\\_FROM\\_SULFURIC\\_ACID\\_SOLUTION\\_ADSORPTION\\_AND\\_KINETICS\\_CHARACTERISTICS](https://www.researchgate.net/publication/328062508_ANION_EXCHANGE_OF_URANIUM_FROM_SULFURIC_ACID_SOLUTION_ADSORPTION_AND_KINETICS_CHARACTERISTICS). Accessed 23 Dec 2019
- Orabi AH, Rabia K, Elshereafy E, Salem A (2017) Application of commercial adsorbent for rare earth elements—uranium mutual separation and purification. *MediterrJChem* 6:238. <https://doi.org/10.13171/mjc66/01712211014-orabi>
- Afifi SY, Elashry SM, Abo-Aly MM (2017) Alkaline leaching for recovery of uranium and copper from calcareous shale, um bogma formation, g. allouga, southwestern sinai. *Egypt Arab J Nucl Sci Appl* 50:213–228
- Kołodzyńska D, Hubicki Z, Skiba A (2009) Heavy metal ions removal in the presence of 1-hydroxyethane-1,1-diphosphonic acid from aqueous solutions on polystyrene anion exchangers. *Ind Eng Chem Res* 48:10584–10593. <https://doi.org/10.1021/ie901195j>
- Kadous A, Didi MA, Villemin D (2011) Removal of uranium(VI) from acetate medium using Lewatit TP 260 resin. *J Radioanal Nucl Chem* 288:553–561. <https://doi.org/10.1007/s10967-010-0970-1>
- Wołowicz A, Hubicki Z (2012) The use of the chelating resin of a new generation Lewatit MonoPlus TP-220 with the bis-picolylamine functional groups in the removal of selected metal ions from acidic solutions. *Chem Eng J* 197:493–508. <https://doi.org/10.1016/j.cej.2012.05.047>
- Liu Y, Cao X, Le Z et al (2010) Pre-concentration and determination of trace uranium (VI) in environments using ion-imprinted chitosan resin via solid phase extraction. *J Braz Chem Soc* 21:533–540. <https://doi.org/10.1590/S0103-50532010000300020>
- Praveen R, Metilda P, Daniel S, Rao T (2005) Solid phase extractive preconcentration of uranium(VI) using quinoline-8-ol anchored chloromethylated polymeric resin beads. *Talanta* 67:960–967. <https://doi.org/10.1016/j.talanta.2005.04.019>
- Kouraim MN, Hagag MS, Ali AH (2019) Sorption of uranium from radioactive wastes by silicate-neutralised polyacrylic. *Int J Environ Anal Chem.* <https://doi.org/10.1080/03067319.2019.1641600>
- Sartore L, Dey K (2019) Preparation and heavy metal ions chelating properties of multifunctional polymer-grafted silica hybrid materials. *Adv Mater Sci Eng* 2019:1–11. <https://doi.org/10.1155/2019/7260851>
- Massey MS, Lezama-Pacheco JS, Nelson JM et al (2014) Uranium incorporation into amorphous silica. *Environ Sci Technol* 48:8636–8644. <https://doi.org/10.1021/es501064m>
- Zhang S, Li J, Wen T et al (2013) Magnetic  $\text{Fe}_3\text{O}_4@ \text{NiO}$  hierarchical structures: preparation and their excellent As(v) and Cr(vi) removal capabilities. *RSC Adv* 3:2754. <https://doi.org/10.1039/c2ra22495j>
- Shapiro L, Brannock WW (1962) Rapid analysis of silicate, carbonate, and phosphate rocks. *US Geological Survey Bulletin* 114A (Revised Edition): <https://doi.org/10.3133/b1144A>
- Kuppusami Govindaraju, Guy Mevelle, Charles Chouard (1976) Automated optical emission spectrochemical bulk analysis of silicate rocks with microwave plasma excitation. *Anal Chem* 48:1325–1331. <https://doi.org/10.1021/ac50003a018>
- Marczenko Z, Balcerzak M (2000) Principles of Spectrophotometry. In: *Analytical spectroscopy library*. Elsevier, pp 26–38
- Davies W (1964) A rapid and specific titrimetric method for the precise determination of uranium using iron(II) sulphate as reductant. *Talanta* 11:1203–1211. [https://doi.org/10.1016/0039-9140\(64\)80171-5](https://doi.org/10.1016/0039-9140(64)80171-5)
- Mathew KJ, Bürger S, Vogt S et al (2009) Uranium assay determination using Davies and Gray titration: an overview and implementation of GUM for uncertainty evaluation. *J Radioanal Nucl Chem* 282:939–944. <https://doi.org/10.1007/s10967-009-0186-4>
- Cheira MF, Atia BM, Kouraim MN (2017) Uranium(VI) recovery from acidic leach liquor by Ambersep 920U  $\text{SO}_4$  resin: kinetic, equilibrium and thermodynamic studies. *J Radiat Res Appl Sci* 10:307–319. <https://doi.org/10.1016/j.jrras.2017.07.005>
- Cheira MF, Orabi AS, Atia BM, Hassan SM (2018) Solvent extraction and separation of thorium(IV) from chloride media by a

- schiff base. *J Solution Chem* 47:611–633. <https://doi.org/10.1007/s10953-018-0740-1>
33. Blanchard G, Maunaye M, Martin G (1984) Removal of heavy metals from waters by means of natural zeolites. *Water Res* 18:1501–1507. [https://doi.org/10.1016/0043-1354\(84\)90124-6](https://doi.org/10.1016/0043-1354(84)90124-6)
  34. Weber J, Morris JC, Weber W et al (1963) Kinetics of adsorption on carbon from solution. *J Sanit Eng Div A Soc Civil Eng* 89:31–60
  35. Langmuir I (1918) The adsorption of gases on plane surfaces of glass, mica and platinum. *J Am Chem Soc* 40:1361–1403. <https://doi.org/10.1021/ja02242a004>
  36. Freundlich H (1907) Adsorption in solution. *Zeitschrift für Physikalische Chemie*. <https://doi.org/10.1515/zpch-1907-5723>
  37. Das DP, Das J, Parida K (2003) Physicochemical characterization and adsorption behavior of calcined Zn/Al hydrotalcite-like compound (HTlc) towards removal of fluoride from aqueous solution. *J Colloid Interface Sci* 261:213–220. [https://doi.org/10.1016/S0021-9797\(03\)00082-1](https://doi.org/10.1016/S0021-9797(03)00082-1)
  38. Liao X, Shi B (2005) Adsorption of Fluoride on Zirconium(IV)-Impregnated Collagen Fiber. *Environ Sci Technol* 39:4628–4632. <https://doi.org/10.1021/es0479944>
  39. Chaudhary N, Balomajumder C (2014) Optimization study of adsorption parameters for removal of phenol on aluminum impregnated fly ash using response surface methodology. *J Taiwan Inst Chem Eng* 45:852–859. <https://doi.org/10.1016/j.jtice.2013.08.016>
  40. Atia BM, Gado MA, Abd El-Magied MO, Elshehy EA (2019) Highly efficient extraction of uranyl ions from aqueous solutions using multi-chelators functionalized graphene oxide. *Sep Sci Technol*. <https://doi.org/10.1080/01496395.2019.1650769>
  41. Kannamba B, Reddy KL, AppaRao BV (2010) Removal of Cu(II) from aqueous solutions using chemically modified chitosan. *J Hazard Mater* 175:939–948. <https://doi.org/10.1016/j.jhazmat.2009.10.098>
  42. Dong J, Ozaki Y (1997) FTIR and FT-Raman studies of partially miscible poly(methyl methacrylate)/poly(4-vinylphenol) blends in solid states. *Macromolecules* 30:286–292. <https://doi.org/10.1021/ma9607168>
  43. Khalifa ME (1998) Selective separation of uranium using alizarin red S (ARS)-modified anion-exchange resin or by flotation of U-ARS chelate. *Sep Sci Technol* 33:2123–2141. <https://doi.org/10.1080/01496399808545719>
  44. Sid Kalal H, Panahi HA, Hoveidi H et al (2012) Synthesis and application of Amberlite Xad-4 functionalized with alizarin red-s for preconcentration and adsorption of rhodium (III). *J Environ Health Sci Engineer* 9:7. <https://doi.org/10.1186/1735-2746-9-7>
  45. Anirudhan TS, Rijith S (2012) Synthesis and characterization of carboxyl terminated poly(methacrylic acid) grafted chitosan/bentonite composite and its application for the recovery of uranium(VI) from aqueous media. *J Environ Radioact* 106:8–19. <https://doi.org/10.1016/j.jenvrad.2011.10.013>
  46. Atrees MS, Metwally E, Demerdash M, Salem H (2016) Sorption behavior of Pr and Nd upon chitosan benzoyl thiourea derivatives. *J Radiat Res Appl Sci* 9:207–216. <https://doi.org/10.1016/j.jrras.2015.02.004>
  47. Solgy M, Taghizadeh M, Ghodocynejad D (2015) Adsorption of uranium(VI) from sulphate solutions using Amberlite IRA-402 resin: equilibrium, kinetics and thermodynamics study. *Ann Nucl Energy* 75:132–138. <https://doi.org/10.1016/j.anucene.2014.08.009>
  48. Massoud A, Masoud AM, Youssef WM (2019) Sorption characteristics of uranium from sulfate leach liquor by commercial strong base anion exchange resins. *J Radioanal Nucl Chem*. <https://doi.org/10.1007/s10967-019-06770-9>
  49. Semnani F, Asadi Z, Samadfam M, Sepehrian H (2012) Uranium(VI) sorption behavior onto amberlite CG-400 anion exchange resin: effects of pH, contact time, temperature and presence of phosphate. *Ann Nucl Energy* 48:21–24. <https://doi.org/10.1016/j.anucene.2012.05.010>
  50. Ladeira ACQ, Gonçalves CR (2007) Influence of anionic species on uranium separation from acid mine water using strong base resins. *J Hazard Mater* 148:499–504. <https://doi.org/10.1016/j.jhazmat.2007.03.003>
  51. Mattigod SV, Golovich EC, Wellman DM, et al (2010) Uranium Adsorption on Ion-Exchange Resins—Batch Testing
  52. Kosari M, Sepehrian H (2016) Uranium Removal from Aqueous Solution Using Ion-Exchange Resin DOWEX<sup>®</sup> 2x8 in the Presence of Sulfate Anions. *Int J Eng* 29:1677–1683
  53. Cheira FM, El-Didamony AM, Mahmoud FK, Atia BM (2014) Equilibrium and kinetic characteristics of uranium recovery by the strong base ambersep 920U Cl resin. *IOSRJAC* 7:32–40. <https://doi.org/10.9790/5736-07533240>
  54. Balanovsky NV, Koshcheeva AM, Cherednichenko AG (2016) Synthesis and properties of strongly basic acrylate polyfunctional anion-exchange resin for uranium extraction. *Moscow Univ Chem Bull* 71:336–340. <https://doi.org/10.3103/S0027131416050023>
  55. Khawassek YM, Eliwa AA, Haggag EA et al (2017) Equilibrium, kinetic and thermodynamics of uranium adsorption by ambersep 400 SO<sub>4</sub> resin. *Arab J Nucl Sci Appl* 50:100–112
  56. Venkatesan KA, Shyamala KV, Antony MP et al (2008) Batch and dynamic extraction of uranium(VI) from nitric acid medium by commercial phosphinic acid resin, Tulsion CH-96. *J Radioanal Nucl Chem* 275:563–570. <https://doi.org/10.1007/s10967-007-6888-6>

**Publisher's Note** Springer Nature remains neutral with regard to jurisdictional claims in published maps and institutional affiliations.